Proceedings of the ASME 2011 Dynamic Systems and Control Conference
DSCC2011
October 31 - November 2, 2011, Arlington, VA, USA

DSCC2011-6119

Simulation and Experimental Analysis of a Portable Powered Ankle-Foot Orthosis Control

Yifan Li
K. Alex Shorter
Elizabeth T. Hsiao-Wecksler
Department of Mechanical Science and Engineering
University of Illinois
Urbana, 61801
yifanli4@illinois.edu

Timothy Bretl
Department of Aerospace Engineering
University of Illinois
Urbana, 61801
tbretl@illinois.edu

ABSTRACT

A portable powered ankle-foot orthosis (PPAFO) was previously developed using off-the-shelf pneumatic components to explore new opportunities for fluid power in human assist devices. The untethered pneumatically powered ankle-foot orthosis provides both motion control and torque assistance at the ankle via a binary, event-based control scheme that uses solenoid valves. While stable, the binary actuation of the solenoid valves that results from this approach limits the overall performance of the system. This paper addresses the limitations of the current system using a modeling approach for both hardware and control design. Hardware and control configurations were first evaluated using simulations of the modeled PPAFO and shank-foot system during a simplified functional gait task: assistive propulsive torque during stance. These simulations demonstrated that the introduction of a proportional valve and new control architecture resulted in PPAFO performance improvements during the task. These results were then confirmed experimentally with the PPAFO attached to a physical model of a shank and foot.

INTRODUCTION

Ankle foot orthoses (AFOs) are orthotic devices used to correct lower limb gait deficiencies. Sizable populations exist in the United States alone that present with symptoms that could be corrected with AFOs: stroke (8M), spinal cord injuries (1.3M), multiple sclerosis (1M), cerebral palsy (412K), and polio (272K) [1, 2]. The ideal AFO should accommodate the many aspects of gait affected by injury or pathology, while being compact and light weight to minimize the energetic impact to the wearer [3].

Prescription AFOs are generally passive due to the size constrains, since the necessity of power source and actuator for active AFOs always results in increased size. Passive AFOs provide assistance by preventing unwanted foot motion with direct physical resistance [4, 5]. Although the motion control provided by passive AFOs can improve functionality, passive devices have limitations that affect performance. For example, the static nature of passive AFOs can impede gait by restricting movements that the patient is normally capable of attaining. Additionally, these devices are unable to adapt to changing environmental conditions or provide supplemental torque [6].

To address these limitations, we have developed a light-weight, portable powered ankle-foot orthosis (PPAFO) using mostly off-the-shelf components [7, 8]. Pneumatic power was selected because of its high power to weight ratio and low power consumption during static forcing. Currently, the torque assistance is controlled with two solenoid valves using binary (all on or all off), event-based control. Sensor measurements are used to identify events during gait and trigger corresponding valve configurations. Solenoid valves were initially selected for their size, simplicity, low cost, and low electrical power consumption. While this approach does provide supplemental torque assistance, there are limitations with the current system. This paper addresses two of these limitations: (1) the binary control of the solenoid valves does not allow the PPAFO to provide intermediate levels of torque

Copyright © 2011 by ASME

Downloaded From: http://proceedings.asmedigitalcollection.asme.org/ on 09/19/2015 Terms of Use: http://www.asme.org/about-asme/terms-of-use

assistance, and (2) the current control scheme may result in excessive actuation and high pneumatic power consumption, limiting the duration of use.

This paper will address the performance and efficiency limitations related to the solenoid valves through a model-based system analysis of a new proportional valve configuration and improved control design. Hardware and control configurations were evaluated using simulations of the modeled PPAFO and shank-foot system during an idealized functional gait tasks: provide assistive propulsive torque during stance. The results from the simulations were then confirmed experimentally with the PPAFO and a physical model of a shank and foot.

The contributions from this paper are twofold. First, this work provides an illustrative example of how to effectively utilize a well-identified system model to aid hardware design as well as develop and test different control strategies for a robotic assist device. Second, the model of the pneumatic system developed here can be used by other researchers working with pneumatic systems. The remainder of this paper will describe the current PPAFO hardware, present models of the PPAFO system and simplified leg, implement the hardware and control schemes both in simulation and experimentally, and compare the performance of the PPAFO with solenoid and proportional valve configurations during an idealized gait task.

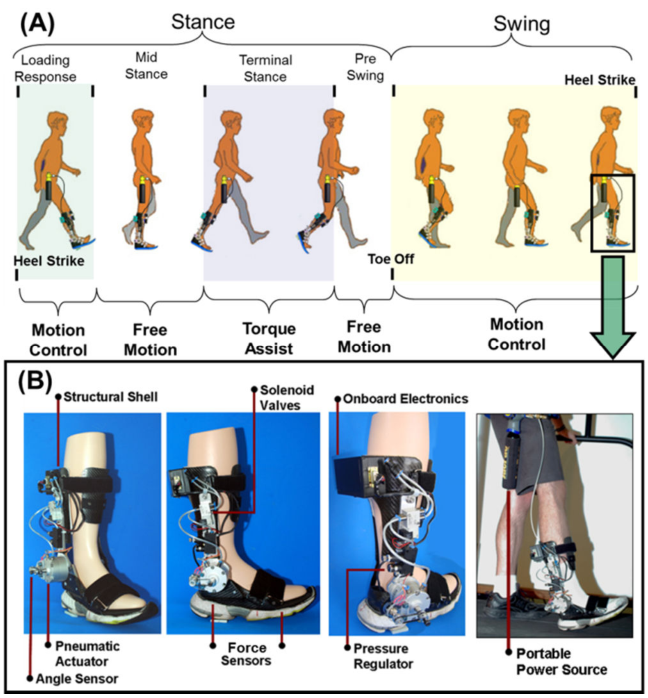

FIGURE 1. *(A) GAIT IS CYCLIC AND SUBDIVIDED INTO MULTIPLE PHASES DEFINED BY FUNCTIONAL TASKS [9]. THE PORTABLE POWERED ANKLE-FOOT ORTHOSIS (PPAFO) ASSISTS GAIT BY CONTROLLING FOOT MOTION AND PROVIDING ASSISTIVE TORQUE FOR PROPULSION. (B) THE PPAFO IS POWERED BY A COMPRESSED CO_2 BOTTLE (FAR RIGHT).*

METHODS

PPAFO Hardware

Walking consists of cyclic motion patterns that are divided into gait cycles beginning and ending at heel strike (Fig. 1A). Lower limb pathology or injury can disrupt the efficiency and effectiveness of all phases of the cycle. The PPAFO assists impaired gait by: (1) controlling the motion of the foot at heel strike, (2) providing modest assistive torque for propulsion and stability during stance, (3) supporting the foot in the neutral (90° joint angle) position during swing to prevent foot-drop, and (4) allowing free range-of-motion during the rest of the cycle (Fig. 1A).

A 255 g (9 oz.) portable compressed liquid CO_2 bottle and pressure regulator (JacPac J-6901-91; Pipeline Inc., Waterloo, Canada) are used to power a dual-vane bidirectional rotary actuator (CRB2BW40-90D-DIM00653; SMC Corp of America, Noblesville, IN, USA) located at the ankle joint (Fig. 1B). Two solenoid valves (VOVG 5V; Festo Corp, Hauppauge, NY) connect the power source to the actuator or vent the CO_2 to atmosphere. The solenoid valves are either fully open or closed and cannot be used to modulate actuator torque. The pressure regulator on the CO_2 bottle and a second regulator (LRMA-QS-4; Festo Corp - US, Hauppauge, NY) located on the PPAFO were used to fix the magnitude of the dorsiflexor (toes-up) and plantarflexor (toes-down) actuator torque.

The structural shell consisted of a tibial section and foot plate, which were custom fabricated from pre-impregnated carbon composite laminate material. A free motion ankle hinge joint connected the foot plate and tibial section on the medial aspect. Velcro straps secure the PPAFO to the shank and foot.

The direction of the PPAFO torque is switched from dorsiflexor (toes-up) to plantarflexor (toes-down) based on valve control. Control of the valves was accomplished through the use of two force sensors, and an angle sensor (force sensor: 2in 2in square; Interlink Electronics Inc., Camarillo, CA, USA; angle sensor: 53 Series; Honeywell, Golden Valley, MN, USA). Onboard electronics (eZ430-F2013 Development Tool; Texas Instruments, Dallas, TX, USA) were used to control the PPAFO. The use of onboard electronics and a portable power source enabled the PPAFO to provide untethered assistance.

While the PPAFO in the above configuration successfully provides assistance during gait (please see reference [7] for details), this system has two previously mentioned limitations: (1) the inability to provide intermediate levels of torque assistance, and (2) excessive actuation and high pneumatic power consumption caused by the current control scheme. To address these issues, a second PPAFO hardware configuration incorporating a single high-speed proportional valve (LS-V05s; Enfield Technologies, Trumbull, CT, USA) in place of the two solenoid valves was considered.

Copyright © 2011 by ASME

Downloaded From: http://proceedings.asmedigitalcollection.asme.org/ on 09/19/2015 Terms of Use: http://www.asme.org/about-asme/terms-of-use

Modeling the PPAFO

The pneumatic system model consists of the proportional valve, rotary actuator, pneumatic lines connecting the valve to the actuator, and the added inertia of the PPAFO foot plate (Fig. 2). The solenoid valve was modeled as a fully open proportional valve with a different cross-sectional area. The inertia and damping of the actuator vane and PPAFO foot plate were modeled as a single rigid body. Additionally, the following assumptions and simplifications were made: constant pressure at the source, no leakage within the system (except for leakage across the actuator vane), homogeneous pressure inside each chamber, negligible gas inertia, isothermal processes, and negligible line losses between the valve and actuator.

In order to determine the angular position of the PPAFO(θ), the dynamics of the system were modeled with the following relationship,

$$I_{zz}\ddot{\theta} + \beta\dot{\theta} + T_{gravity} + T_f + T_{ex} = T_{actuator} \tag{1}$$

In (1), θ is the vane position angle (which corresponds to the ankle joint angle), I_{zz} is the moment of inertia of the foot plate and actuator vane relative to the ankle joint axis of rotation, β is the rotary damping ratio due to friction, $T_{gravity}$ is the gravitational torque due to the weight of the PPAFO, T_{ex} represents the coupling torque between the PPAFO and the wearer, T_f is the frictional torque opposing the motion of the vane, and $T_{actuator}$ is the output torque created by the actuator (Fig. 2).

The actuator torque was calculated using the following equation [10]:

$$T_{actuator} = (P_1 - P_2)K_{actuator} \tag{2}$$

where $K_{actuator}$ is an experimentally derived torque-to-pressure ratio for the rotary actuator, and P_i are the pressures in the two actuator chambers. The instantaneous pressure in chamber i was calculated using the ideal gas law,

$$P_i = \frac{m_i}{V_i M} RT \tag{3}$$

In (3), V_i is volume of the actuator chamber and the pneumatic lines from the valve, m_i is the mass of CO_2 in the chamber and pneumatic lines, M is the molecular weight of CO_2 (44 g/mol), R is the universal gas constant (8.314 J/(K·mol)), and T is the temperature of the gas (room temperature, due to isothermal assumption). The chamber volume depends linearly on the vane angle:

$$V_1 = B_{vane}\theta \tag{4}$$

$$V_2 = B_{vane}\left(\frac{\pi}{2} - \theta\right) \tag{5}$$

In (5), B_{vane} is the volume to angle ratio for the rotary actuator. The mass of CO_2 in each actuator chamber at a given time determines the resulting pressure. The initial mass values were calculated from initial pressure (atmosphere), and mass flow rates were numerically calculated. Orifice plate flow theory was used to simplify and model the mass flow rate [11]. The mass flow into and out of the actuator chambers were driven by pressure differentials within the system and were divided into two regimes:

choked flow $\frac{P_{up}}{P_{dn}} > (\frac{k+1}{2})^{\frac{k}{k-1}} = 1.832$.

and non-choked flow $\frac{P_{up}}{P_{dn}} < (\frac{k+1}{2})^{\frac{k}{k-1}} = 1.832$

where k = 1.3 for CO_2, and P_{up} and P_{dn} are upstream and downstream pressure. When the choked flow condition was satisfied, the mass flow rate was defined as,

$$\dot{m} = f(P_{up}, P_{dn}, A) = C_d A C_1 P_{up} \tag{6}$$

where $C_1 = \sqrt{\frac{kM}{RT}\left(\frac{2}{k+1}\right)^{(k+1)/(k-1)}} = 0.00281$, C_d is the discharge coefficient, and A is the cross-sectional area for either the proportional or solenoid valve (A_{valve}) or the leakage across the vane (A_{leak}). When the non-choke condition was satisfied, the mass flow rate was defined as:

$$\dot{m} = C_d A C_2 P_{up}\left(\frac{P_{dn}}{P_{up}}\right)^{\frac{1}{k}}\sqrt{1-\left(\frac{P_{dn}}{P_{up}}\right)^{\frac{(k-1)}{k}}} \tag{7}$$

where $C_2 = \sqrt{\frac{2kM}{RT(k-1)}}$ = 0.0124 Thus, $\dot{m}$ described the mass flow rate as a function of upstream pressure P_{up}, downstream pressure P_{dn}, and the cross sectional area of flow restrictions [11]. Again, the coefficient A describes the equivalent cross-sectional area for either the proportional or solenoid valve (A_{valve}) or the leakage across the vane (A_{leak}). For a given valve, the values for the cross-sectional areas were the same for equations (6) and (7). In our system, we had mass flow from the source through the valve into the actuator ($\dot{m}_{in}$, leakage across the actuator vane (, and flow out of the actuator (, such that:

$$\dot{m}_{out} = f(P_2, P_{atm}, A_{valve}), \tag{8a}$$

$$\dot{m}_{in} = f(P_{source}, P_1, A_{valve}), \tag{8b}$$

$$\dot{m}_{leak} = f(P_1, P_2, A_{leak}), \tag{8c}$$

$$\dot{m}_1 = \dot{m}_{in} - \dot{m}_{leak}, \tag{9a}$$

$$\dot{m}_2 = -\dot{m}_{out} + \dot{m}_{leak}, \tag{9b}$$

In these equations, P_{source} was the pressure from the supply (CO_2 bottle), A_{valve} is the cross-section area of the valve orifice, (this value differed between valves), and A_{leak} is the equivalent cross-section area of the leakage pathway across the actuator vane.

Copyright © 2011 by ASME

Downloaded From: http://proceedings.asmedigitalcollection.asme.org/ on 09/19/2015 Terms of Use: http://www.asme.org/about-asme/terms-of-use

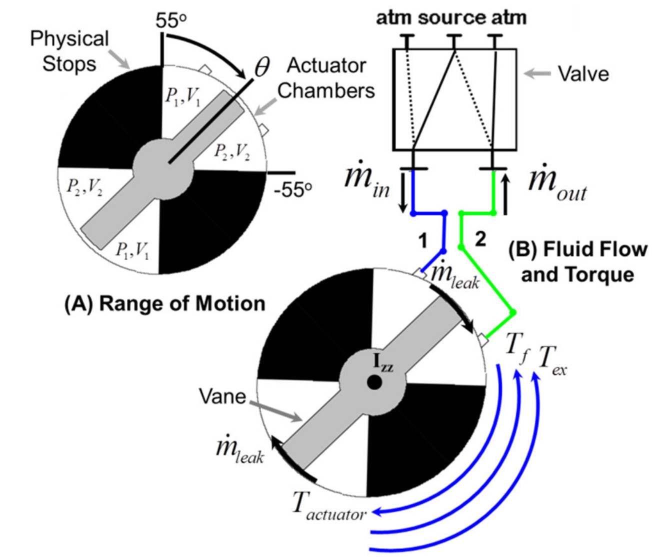

FIGURE 2. *THE MODELED PPAFO PNEUMATIC ACTUATION SYSTEM CONSISTS OF A DUAL-VANE ROTARY ACTUATOR, SOLENOID OR PROPORTIONAL VALVE, AND PNEUMATIC LINES. THE PRESSURE DIFFERENTIAL ACROSS THE VANE THAT DRIVES THE SYSTEM WAS CONTROLLED BY THE VALVES. ADDITIONAL SYMBOLS DEFINED IN THE TEXT.*

Finally, the Coulomb friction torque T_f can be expressed as,

$$T_f = \begin{Bmatrix} T_{f,static} & \text{if } \dot{\theta} = 0 \\ -sign(\dot{\theta}) \cdot T_{f,dynamic} & \dot{\theta} \neq 0 \end{Bmatrix} \quad (10)$$

In (10), $T_{f,static}$ is the static frictional torque that opposes the net torque applied on the actuator with an experimentally determined maximum ($T_{f,static,max}$). The dynamic friction, $T_{f,dynamic}$, also opposes the motion of the vane with sign( ) determined accordingly.

Identification of PPAFO Model Parameters

Parameters for the model described in equations (1-10) were identified from indirect and direct experimental measurements, 3D modeling software, and component data sheets.

The actuator torque/pressure constant ($K_{actuator}$), the static and dynamic frictional torque of the actuator ($T_{f,static,max}$ and $T_{f,dynamic}$), and β were determined experimentally. To identify the parameter $K_{actuator}$, static force measurements were made using a digital scale (Berkley, IA, USA) over a 95 psig range. Three repetitions of measurements were made at increasing and decreasing 5 psig increments (Fig. 3 left panel). The difference between the increasing and decreasing measurements was a result of static friction. As pressure increased (×), static friction opposed vane motion reducing force measurements at the scale. The opposite effect occurred as pressure was decreased from 95 psig (○) resulting in higher force measurements. The torque difference between data points at equivalent pressures was twice the static frictional torque of the actuator ($T_{f,\ static,max}$= 0.45Nm). The nominal actuator torque (solid line) lies between the data points. The slope of this line was defined as the actuator torque/pressure constant ($K_{actuator}$=1.451×10^{-5} m^3).

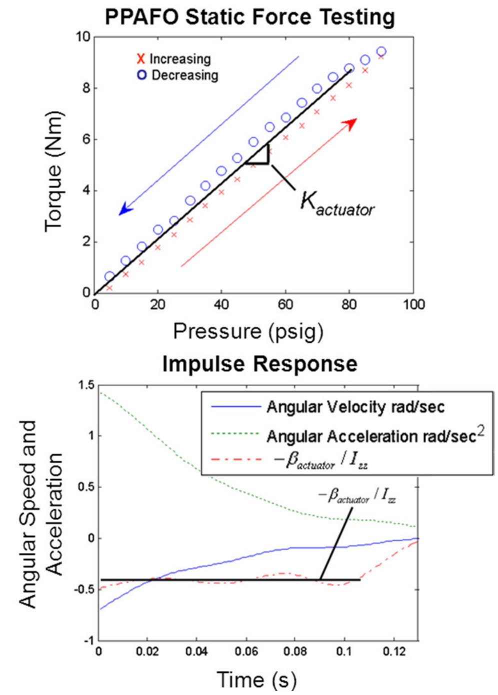

FIGURE 3. *TOP PANEL: EXPERIMENTAL DETERMINATION OF $K_{actuator}$. ACTUATOR PRESSURE WAS INCREMENTED EVERY 5 PSIG FROM 0 PSIG TO 95 PSIG AND THEN BACK TO 0 PSIG. BOTTOM PANEL: EXPERIMENTAL DETERMINATION OF ROTARY DAMPING RATIO $\beta_{actuator}$.*

The PPAFO rotary damping ratio β was determined through a multi-step process. First, the system was positioned horizontally to reduce the gravitational force acting on the foot plate. Next, an impulsive force was applied to the end of the foot plate. The resulting angular motion was recorded using the AFO angle sensor, and the ratio between the angular velocity (ω) and acceleration (α) was ω/α=-β/I_{zz} (average at -0.4/sec) (Fig. 3 right panel). β was then obtained by multiplying the ratio by the system moment of inertia I_{zz} (β =32 g m^2/s). The moment of inertia of the actuator and foot plate (I_{zz} =8.4g m^2) was estimated from a 3D CAD model of the components (Autodesk Inventor 2010, Autodesk, Inc. San Rafael, CA). Losses due to dynamic friction at velocities close to zero were then found using, $T_{f,\ dynamic}$=-$I_{zz}\alpha$, with α=0.13rad/s^2. It was then calculated that $T_{f,\ dynamic}$=0.011Nm.

Direct measurement of the fully open flow rate (=1.5g/sec at 50psig) through the valves was used to determine C_d=0.113sec/m for the solenoid (A_{valve}=12.6 mm^2) and proportional (A_{valve}=31.6 mm^2) valves in equations 9 and 10. The mass flow rate of the leakage across the actuator vane, $\dot{m}$ = 0.045g/sec, and the cross sectional area of the

Copyright © 2011 by ASME

Downloaded From: http://proceedings.asmedigitalcollection.asme.org/ on 09/19/2015 Terms of Use: http://www.asme.org/about-asme/terms-of-use

leakage pathway, A_{leak}=0.3 mm^2, were identified through direct measurement of the mass flow rate across the vane.

Finally, the volume to angle ratio of the actuator vane (B_{vane}=51 cm^3/rad) was taken from the actuator data sheet. The CO_2 was assumed to be at room temperature (T = 298 K) and at a source pressure of P_{source}=50psig.

Simplified model of the leg

A simple planar two-link rigid body pendulum was used to represent the foot and shank segments of the leg (Fig 4A). The motion of the model was confined to the sagittal plane, and two degrees of freedom defined allowable configurations: the segment angle of the shank ( ), and the ankle joint angle (θ). Note that the motion of both the angular position of the PPAFO vane/foot plate and the ankle joint angle of the model leg are described by θ. The dynamics of the leg model were derived from the Euler-Lagrange formulation [12],

$$\mathbf{M(q)\ddot{q}} + \mathbf{C(\dot{q},q)\dot{q}} + \mathbf{G(q)} = \begin{Bmatrix} T_1 \\ T_2 + T_{ex} \end{Bmatrix} \qquad (11)$$

$$\text{where } \mathbf{q} = \begin{Bmatrix} \phi \\ \theta \end{Bmatrix} \qquad (12)$$

In (11), $M(q,\dot{q})$ is the inertia matrix, $C(q,\dot{q})$ contains the centrifugal and Coriolis terms, $G(\boldsymbol{q})$ is the gravity vector, T_1 is the knee joint torque, T_2 is the ankle joint torque, and T_{ex} is the torque applied to the leg model from the PPAFO, which is the same coupling torque in equation (1). The physical parameters of the model are based on anthropometric measurements from a single subject (72.5 kg, 1.9 m young adult male): l_{shank} = 0.46 m, l_{foot} = 0.18 m, m_{shank} = 4.5 kg, m_{foot} = 1.0 kg, $I_{zz,\ shank}$ = 0.1 kg m^2 and $I_{zz,\ foot}$ = 0.001kg m^2. Experimental kinematic walking data without the PPAFO from the same subject were used to calculate the shank segment motion, ϕ and . The experimental protocol was approved by the institutional review board and informed consent was obtained.

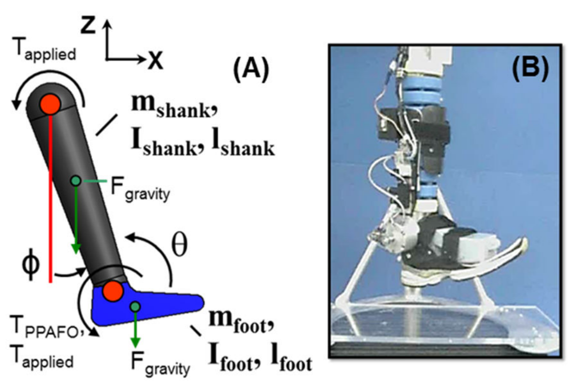

FIGURE 4. ***(A)*** *THE TWO-LINK RIGID BODY LEG MODEL IS COUPLED TO THE PPAFO THROUGH THE APPLIED EXTERNAL TORQUE* T_{ex}. ***(B)*** *THE EXPERIMENTAL TEST FIXTURE AND PPAFO.*

Because the motion of the shank was prescribed, the knee joint torque (T_1) was determined by the experimental data. For the model simulations, we assumed that the ankle joint torque from the individual was zero (T_2=0), simulating a 100% deficit. This assumption was reasonable because a low friction mechanical joint approximated the ankle joint on the test fixture used during experimental testing (Fig. 4B). The nominal impedance of the tendons and soft tissue of the ankle joint should be considered in future work. The PPAFO was used to control the motion of the foot through the applied torque T_{ex}. Equations (1) and the second equation (describing the motion of the foot) from (11) were then used to determine θ.

Simulation and Experimental Analysis

Two different analyses were performed. The first was an experimental validation of the model using the PPAFO on a test fixture. The second was to compare in simulation and experimentally the performance of the PPAFO with solenoid and proportional valve configurations during an idealized gait task.

Experimental Model Validation. After formulating the mathematical models and identifying system parameters, an experimental validation was conducted using a test fixture. The test fixture consisted of a rigid aluminum stand and a physical model of a shank and foot with rotational freedom at the ankle and knee joints (Fig 4B). The inertial properties of the physical model of the leg were based on the same anthropometric data used to determine the parameters for the shank-foot model. A test fixture was used because it provided a more controlled environment for the system evaluation than a human subject.

Experimental data collected from the PPAFO on the test fixture during a pressure step response was compared to simulated data to validate the coupled PPAFO-leg model. Only the proportional valve was considered because the solenoid valve was essentially the same system with a different parameter (orifice cross-sectional area). A step response was selected for the analysis because it is typical of the simplified functional task that will be used to evaluate system performance. For both system configurations, the source pressure was set to 55 psig, and the PPAFO moved across the entire 110 deg range of motion. Experimental joint angle data and pressure data from two external transducers (pressure transducer: 4100 series; American Sensor Technology, Mt. Olive, NJ, USA) were collected to validate the simulation results.

Task assessment. To compare the performance of the two hardware configurations, a simplified torque control task was defined (Fig. 5). In this task, the PPAFO provided assistive plantarflexor torque for propulsion assistance during stance. The PPAFO was used to track a torque profile consisting of a ramp and hold function.

This simplified profile emulated the behavioral trend seen in torque profiles from healthy walkers. For simplification of the model dynamics, the entire foot segment remained in

Copyright © 2011 by ASME

Downloaded From: http://proceedings.asmedigitalcollection.asme.org/ on 09/19/2015 Terms of Use: http://www.asme.org/about-asme/terms-of-use

contact with the ground for the duration of the task, and the test fixture shank motion was generated manually. Because of the way this task has been defined the dynamics of the simplified leg model do not contribute to the coupled system dynamics. However, these dynamics would be present during other tasks like controlling the motion of the foot during swing.

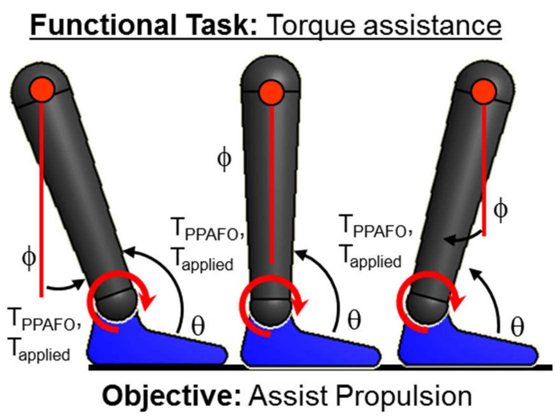

FIGURE 5. *THE PERFORMANCE AND EFFICIENCY OF PPAFO HARDWARE CONFIGURATIONS AND CONTROL ALGORITHMS WERE EXAMINED DURING A SIMPLIFIED FUNCTIONAL TASK: PROPULSIVE TORQUE (RED CIRCULAR ARROW) ASSIST DURING STANCE.*

PPAFO Control During the Task Assessment. The second analysis task, in which the performance of the PPAFO with the proportional and solenoid valve configurations was compared, required the use of two different control schemes. These two approaches are presented below.

A PID controller was used to control the proportional valve during the functional task. This type of control was selected for simplicity and ease of implementation. The control signal U_{Pro} was determined as,

$$U = k_p + k_i \frac{1}{s} + k_d s \tag{13}$$

where k_p is the proportional gain, k_i is the integral gain and k_d is the derivative gain (Fig 6). These gains were heuristically tuned to minimize the tracking error during the task. The same gains were used to generate both simulated and experimental results: $k_p = 0.095$, $k_i = 0.25$, and $k_d = 0.006$.

The solenoid valves were controlled in a binary manner, where the input control voltage to the valves was driven by a digital on/off signal. Since the two solenoid valves were controlling opposite sides of the rotary actuator, the control signals were always out of phase. The control signals for the two solenoid valves (U_A and U_B) were generated by a simple rule: if the error e was greater or equal than zero, trigger only valve A (setting it to +5 Volts) otherwise trigger only valve B. A dead-zone was not implemented with this system because the slow switching time of the valves created a large delay that would have been amplified by an additional dead-zone.

$$U_{sol} = \begin{cases} e \geq 0 & U_A = +5 \\ & U_B = 0 \\ e < 0 & U_A = 0 \\ & U_B = +5 \end{cases} \tag{14}$$

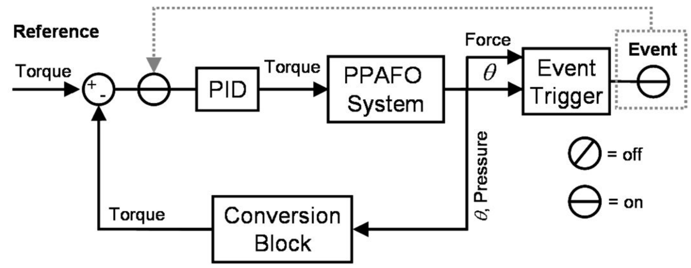

FIGURE 6. *A PID FEEDBACK CONTROLLER WAS USED TO TRACK THE TORQUE REFERENCE TRAJECTORY DURING THE FUNCTIONAL TASK. NOTE THAT WHEN IMPLEMENTED ON THE PPAFO WITH AN IMPAIRED SUBJECT, THE CONTROL SCHEME WOULD BE EVENT DRIVEN. ASSISTIVE TORQUE WOULD BE APPLIED DURING SPECIFIC REGIONS OF THE GAIT CYCLE. THE BOUNDARIES OF THESE REGIONS WOULD BE DETERMINED BY EVENTS DURING THE CYCLE.*

RESULTS

PPAFO Model Validation

During the experimental validation of the model, similar trends between simulation and experiment were observed in the position and pressure response. The displacement of the vane, pressure in both chambers and the pressure difference across the vane are shown in Fig. 7.

As can be seen from the figure, the pressure initially increased inside Chamber 1 until the vane's maximum static friction ($T_{static,max}$) was exceeded and the vane began to move (Fig. 7A). At this point, the pressure in Chamber 1 decreased as the volume V_1, was increased by the moving vane (Fig. 7C). After the vane stopped rotating, the pressure in Chamber 1 increased to the source pressure. The pressure in Chamber 2 (Fig. 7 D), initially at the source pressure, began to decrease when the valve was opened. As the vane moved, the rate at which the pressure was dropping briefly slowed. This rate reduction was due to the compression of the CO_2 in Chamber 2, which occurred briefly before equalizing to atmospheric pressure.

The agreement between model-predicted and experimental results for the PPAFO are of particular note because they illustrate the fidelity of the model. During the step response, the root mean square (RMS) errors between the simulation and the experimental results for the vane position and pressure were within an acceptable range (10% of the full range): vane position (2.1 deg, 1.9% of the full range: 110 deg), pressure in chamber 1 (3.7 psi, 6.8% of the full range: 55 psi), pressure in

 Copyright © 2011 by ASME

Downloaded From: http://proceedings.asmedigitalcollection.asme.org/ on 09/19/2015 Terms of Use: http://www.asme.org/about-asme/terms-of-use

chamber 2 (1.4 psi, 2.6% of the full range: 55 psi) and pressure difference (4.8 psi, 4.4% of the full range: 110 psi).

The differences between the predicted and experimental response of the pressure are due to the potential presence of unmodeled system dynamics, such as higher-order dynamics and resonances that were not captured by the simplified model. Additionally, taking changes in CO_2 temperature into account could also improve model accuracy.

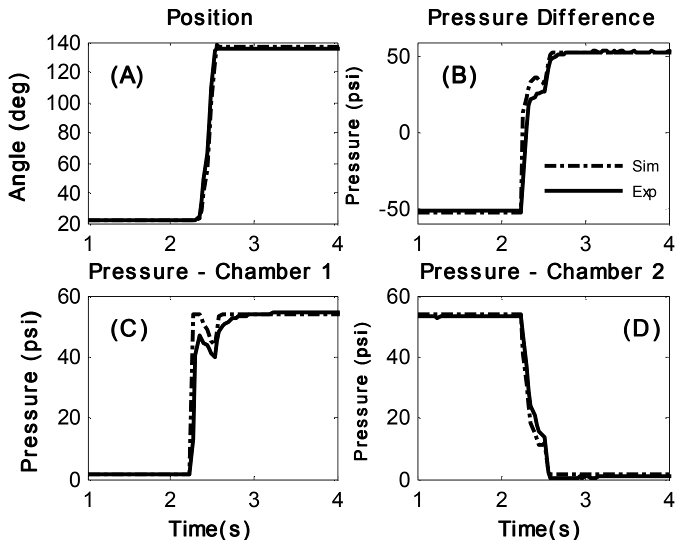

FIGURE 7. *SIMULATED AND EXPERIMENTAL STEP RESPONSE OF THE PPAFO SYSTEM CONFIGURED WITH THE PROPORTIONAL VALVE: (A) VANE ANGLE INCREASED FROM 20 TO 130 DEG. (B) PRESSURE DIFFERENCE BUILT UP AS THE FLOW SWITCHED. (C) PRESSURE RESPONSE GREW IN THE FIRST CHAMBER (P_1). (D) PRESSURE (P_2) IN THE SECOND CHAMBER FELL AS THE VANE ROTATED.*

Task Assessments

The simulated task assessments demonstrated that the proportional valve outperformed the solenoid valves during the simplified functional task (Fig. 8). In the task, the PPAFO was used to provide an assistive plantarflexor torque for propulsion assistance during stance. The proportional valve had a 15% improvement in RMS tracking error over the solenoid valve. Additionally, the oscillatory behavior displayed by the solenoid valves during the initial ramp portion of the trajectory illustrated poor system performance that would not be desirable during actual implementation with an impaired subject, Fig. 8 top panel. The experimental results also found that the proportional valves had lower CO_2 consumption (63% less) than the solenoid valve (from 1.1 g, to 0.4 g).

DISCUSSION

In this work, a model-based system analysis approach was selected to enhance the researcher's ability to implement new hardware and control algorithms for a pneumatic robotic assist device, the PPAFO. This design approach was selected because it provides access to information that might be unavailable in a purely experimental evaluation of the system. System modeling also enables the designer to quickly evaluate performance in a safe yet relatively accurate virtual environment, reducing effort for both system hardware selection and control design.

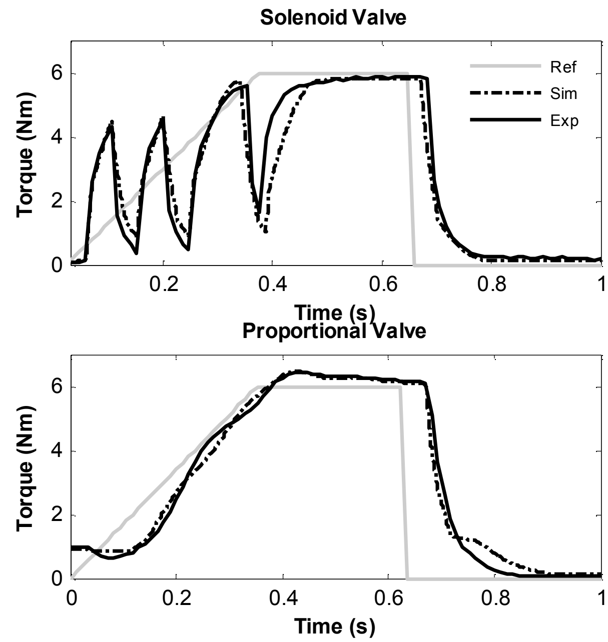

FIGURE 8. *EXPERIMENTAL AND SIMULATION RESULTS FOR BOTH VALVE CONFIGURATIONS DURING THE SIMPLIFIED FUNCTIONAL TASK. THE SYSTEM CONFIGURED WITH THE PROPORTIONAL VALVE (BOTTOM PANEL) TRACKED THE REFERENCE TRAJECTORY BETTER THAN THE SOLENOID VALVE (TOP PANEL), PARTICULARLY DURING THE INITIAL RAMP.*

Accordingly, the PPAFO system model derived in this work was used to design control architectures and to compare the performance of the system with two pneumatic valve configurations: the current solenoid valves and a new proportional valve. The implementation of a proportional valve and new control methodology addressed two identified system limitations: (1) an inability to generate intermediate levels of torque for assistance and motion control, and (2) high pneumatic power consumption caused by inefficient actuation.

The performance benefits from the proportional valve were highlighted by the results from the simulated functional task. Unlike the solenoid valves, the proportional valve has the functional capability to modulate system torque to track a changing reference. The proportional valve was also significantly more efficient, consuming 63% less CO_2 during the task. The performance of the solenoid valves were severely limited by the component-driven 20 Hz switching frequency. The slow switching introduced significant delays that resulted in oscillatory behavior during the task, particularly during the ramp tracking, that cannot be overcome with improved control alone.

Copyright © 2011 by ASME

Downloaded From: http://proceedings.asmedigitalcollection.asme.org/ on 09/19/2015 Terms of Use: http://www.asme.org/about-asme/terms-of-use

Despite these performance advantages, there are functional disadvantages such as the relatively large size and weight characteristics of the valve and control electronics for the proportional valve when compared to the solenoid valve that must be considered. Future work will be directed towards the experimental evaluation of the modified PPAFO system with subjects.

CONCLUSION

Accurate models facilitate the design of system hardware and control schemes that maximize the benefit that a user derives from a robotic assist device. This work has resulted in a well-identified model of a pneumatic robotic assist device, the portable powered ankle-foot orthosis. This model was used to enhance the analysis of a new valve configuration and a modified control scheme to address limitations in the current PPAFO system configuration. The results of this analysis demonstrated that the improvements to the PPAFO system presented here have the potential to significantly improve the performance and efficiency of the device. These improvements are crucial to transitioning the PPAFO system from a laboratory tool into a practical human assist device.

REFERENCES

[1] "One Degree of Separation: Paralysis and Spinal Cord Injury in the United States". 2009, Christopher and Dana Reeve Foundation.

[2] Roger, V.L., et al., Heart disease and stroke statistics-2011 update: A report from the American Heart Association. Circulation. 123(4): p. e18-e19.

[3] Waters, R. L., and Mulroy, S., 1999, "The energy expenditure of normal and pathologic gait," Gait & Posture, 9 (3), pp. 207-231.

[4] Redford, J. B., 1986, Orthotics etcetera., Williams and Wilkins, Baltimore, MD.

[5] Rose, G. K., 1986, Orthotics: Principles and Practice, Williams Heinemann, London.

[6] Svensson, W., and Holmberg, U., "Ankle-foot-orthosis control in inclinations and stairs," Proc. 2008 IEEE International Conference on Robotics, Automation and Mechatronics, pp. 301-306.

[7] Shorter, K. A., Hsiao-Wecksler, E. T., Kogler, G. F., Loth, E., and Durfee, W. K., Accepted 2010, "A Portable-Powered-Ankle-Foot-Orthosis for rehabilitation," Journal of Rehabilitation Research & Development.

[8] Hsiao-Wecksler, E. T., Loth, E., Kogler, G., Shorter, K. A., Thomas, J. A., and Gilmer, J. N., 2009, "Portable powered ankle-foot-orthosis," U. S. P. Office, ed, 12/898,519.

[9] Perry, J., 1992, Gait analysis: normal and pathological function, Slack INC., Thorofare, NJ.

[10] Richer, E., and Hurmuzlu, Y., 2000, "A High Performance Pneumatic Force Actuator System: Part I—Nonlinear Mathematical Model," Journal of Dynamic Systems, Measurement, and Control 122(3), pp. 416-426.

[11] Munson, B. R., Young, D. F., and Okiishi, T. H., 1990, Fundamentals of Fluid Mechanics, Wiley, New York.

[12] Spong, M., Hutchinson, S., and Vidyasagar, M., 2006, Robot Modeling and Control, John Wiley & Sons.

Copyright © 2011 by ASME

Downloaded From: http://proceedings.asmedigitalcollection.asme.org/ on 09/19/2015 Terms of Use: http://www.asme.org/about-asme/terms-of-use